

ORIGINAL ARTICLE

Oncogenic pathways impinging on the G₂-restriction pointF Fojier^{1,2}, M Simonis³, M van Vliet^{1,4}, L Wessels^{1,4}, R Kerkhoven³, PK Sorger² and H te Riele¹

¹Division of Molecular Biology, The Netherlands Cancer Institute, Amsterdam, The Netherlands; ²Department of Systems Biology, Harvard Medical School, Boston, MA, USA; ³Central Microarray Facility, The Netherlands Cancer Institute, Amsterdam, The Netherlands and ⁴Faculty of Electrical Engineering, Mathematics and Computer Science, Delft University of Technology, Delft, The Netherlands

In the absence of mitogenic stimuli, cells normally arrest in G_{1/0}, because they fail to pass the G₁-restriction point. However, abrogation of the G₁-restriction point (by loss of the retinoblastoma gene family) reveals a second-restriction point that arrests cells in G₂. Serum-starvation-induced G₂ arrest is effectuated through inhibitory interactions of p27^{KIP1} and p21^{CIP1} with cyclins A and B1 and can be reversed through mitogen re-addition. In this study, we have investigated the pathways that allow cell cycle re-entry from this G₂ arrest. We provide evidence that recovery from G₂ arrest depends on the rat sarcoma viral oncogene (RAS) and phosphatidylinositol-3 kinase pathways and show that oncogenic hits, such as over-expression of c-MYC or mutational activation of RAS can abrogate the G₂-restriction point. Together, our results provide new mechanistic insight into multistep carcinogenesis.

Oncogene (2008) 27, 1142–1154; doi:10.1038/sj.onc.1210724; published online 13 August 2007

Keywords: mitogenic signaling; G₂ restriction point; retinoblastoma gene family; expression profiling; c-MYC; RAS

Introduction

Cellular proliferation critically depends on the presence of mitogenic stimuli. In the absence of these stimuli, normal cells fail to progress through the G₁-restriction point and arrest in the G_{1/0} phase of the cell cycle (for recent review see Blagosklonny and Pardee, 2002; Fojier and te Riele, 2006b). Decreased phosphatidylinositol (PI)-3 kinase and rat sarcoma viral oncogene (RAS) activity cause cyclin D protein level to be reduced (Malumbres and Barbacid, 2001). Additionally, loss of PI-3 kinase activity activates the Forkhead transcription factor, which stimulates transcription of the CDK1/2 inhibitor (CKI) p27^{KIP1} (Medema *et al.*, 2000). The absence of cyclin D and inhibition of cyclin E/CDK2

results in hypophosphorylation of the retinoblastoma protein family (pRb, p107 and p130, also known as the pocket proteins), inhibition of E2F transcription factors and cell-cycle arrest in G_{1/0} (Fojier and te Riele, 2006a).

However, when the retinoblastoma family is absent or inactivated, a frequent event in human cancer (Malumbres and Barbacid, 2001), cell proliferation is still dependent on mitogens. We have previously shown that serum starvation of *Rb*^{-/-}*p107*^{-/-}*p130*^{-/-} (triple knockout, TKO) mouse embryonic fibroblasts (MEFs) resulted in substantial apoptosis (Dannenberg *et al.*, 2000; Sage *et al.*, 2000) while surviving cells arrested in G₂ (Fojier *et al.*, 2005). TKO MEFs expressing the antiapoptotic protein B-cell lymphoma 2 (BCL2) (TKO-BCL2 MEFs) all arrested in G₂. Serum-starvation-induced G₂ arrest was not restricted to TKO-BCL2 MEFs: partial pocket protein inactivation, either through loss of one or two pocket proteins or oncogene-mediated inhibition resulted in partial G₂ arrest. Serum-starvation-induced G₂ arrest in TKO-BCL2 cells occurred through accumulation of p27^{KIP1} and p21^{CIP1} (Fojier *et al.*, 2005). Both CKIs have previously been shown to be potent inhibitors of CDK2 and CDK1 activity (Harper *et al.*, 1993; Toyoshima and Hunter, 1994; Smits *et al.*, 2000b; Baus *et al.*, 2003; Nakayama *et al.*, 2004; Aleem *et al.*, 2005). In serum-starved TKO-BCL2 MEFs, they effectuated G₂ arrest through direct association with the mitotic kinases cyclin A-CDK2 and cyclin B1-CDK1. The G₂ arrest could be maintained over several weeks but was reversible: serum stimulation led to decreased levels of p27^{KIP1} and p21^{CIP1}, increased activity of cyclin A- and B1-associated kinases and synchronous entry into mitosis (Fojier *et al.*, 2005). This G₂ arrest behaved as a true restriction point as the presence of mitogens was required for only a limited period of time: after 3–6 h of mitogen stimulation, cells could progress through the remainder of G₂ independently of serum and entered mitosis 10 h thereafter (Fojier and te Riele, 2006b). In TKO MEFs, in which p53 was inhibited by RNA interference (TKO-p53RNAi MEFs), p21^{CIP1} and p27^{KIP1} failed to accumulate, allowing unconstrained proliferation under mitogen-deprived conditions (Fojier *et al.*, 2005). Thus, the G₂-restriction point seems to function as a p53-dependent emergency brake that prevents unconstrained proliferation when pocket protein activity is absent or compromised.

Correspondence: Professor H te Riele, Division of Molecular Biology, The Netherlands Cancer Institute, Plesmanlaan 121, 1066 CX, Amsterdam, The Netherlands.
E-mail: h.t.rielle@nki.nl

Received 3 November 2006; revised 15 June 2007; accepted 10 July 2007; published online 13 August 2007

In this study, we have made a survey of the molecular pathways that are involved in cell-cycle re-entry after serum stimulation of G₂-arrested cells by expression profiling. We show that the serum response of G₂-arrested cells is very similar to the response of G₁-arrested cells. In addition, we have studied the involvement of known mitogen-induced pathways in cell-cycle re-entry using chemical inhibition. Finally, we have identified oncogenic events that can disrupt the G₂-restriction point, resulting in mitogen-independent growth.

Results

Expression profiling of G₂-arrested cells re-entering the cell cycle

Serum-starved TKO-BCL2 MEFs can synchronously re-enter the cell cycle upon serum stimulation (Foijer *et al.*, 2005). To gain more insight into the pathways that are involved in cell-cycle re-entry from the G₂ arrest, we have determined the expression profile of serum-stimulated TKO-BCL2 MEFs as a function of time. We analysed 26 time points, ranging from 10 min to 48 h after serum stimulation, with the majority of time points before mitotic entry (at 15 h). The expression pattern of 24878 genes was determined by hybridizing a mixture of Cy 5-dye-labeled amplified RNA generated from

re-stimulated cells and Cy 3-dye-labeled reference amplified RNA from asynchronously proliferating TKO-BCL2 MEFs to 32K mouse oligo-microarrays. Raw data were Lowess normalized (Yang *et al.*, 2002) and for all time points hybridizations were performed in duplicate using dye-swap to minimize dye bias artifacts. Expression values were normalized for expression under serum-starved conditions ($t=0$). From this data set, we selected probes that showed a significant change of expression ($P<0.01$) compared to the reference cDNA at three time points or more. This yielded a data set containing 8691 unique probes.

To verify the quality of the microarray data, we performed qPCR analysis for four genes (Figure 1, bars) and compared this to the expression profiles from the microarray data (Figure 1, lines). The microarray expression profiles and qPCR data were very similar for genes that showed a strong change in expression (*c-Fos* and *c-Jun*; Figures 1a and b) and a very good correlation for genes that showed a more modest change in expression like *p21^{CIP1}* (Figure 1c) and *cyclin B1* (Figure 1d). This indicates that the microarray data of the serum-stimulated TKO-BCL2 MEFs were of sufficient quality for further analyses.

Expression profiles as a function of time

Serum stimulation of G₁-arrested cells resulted in several transcriptional responses that differed over time (Iyer

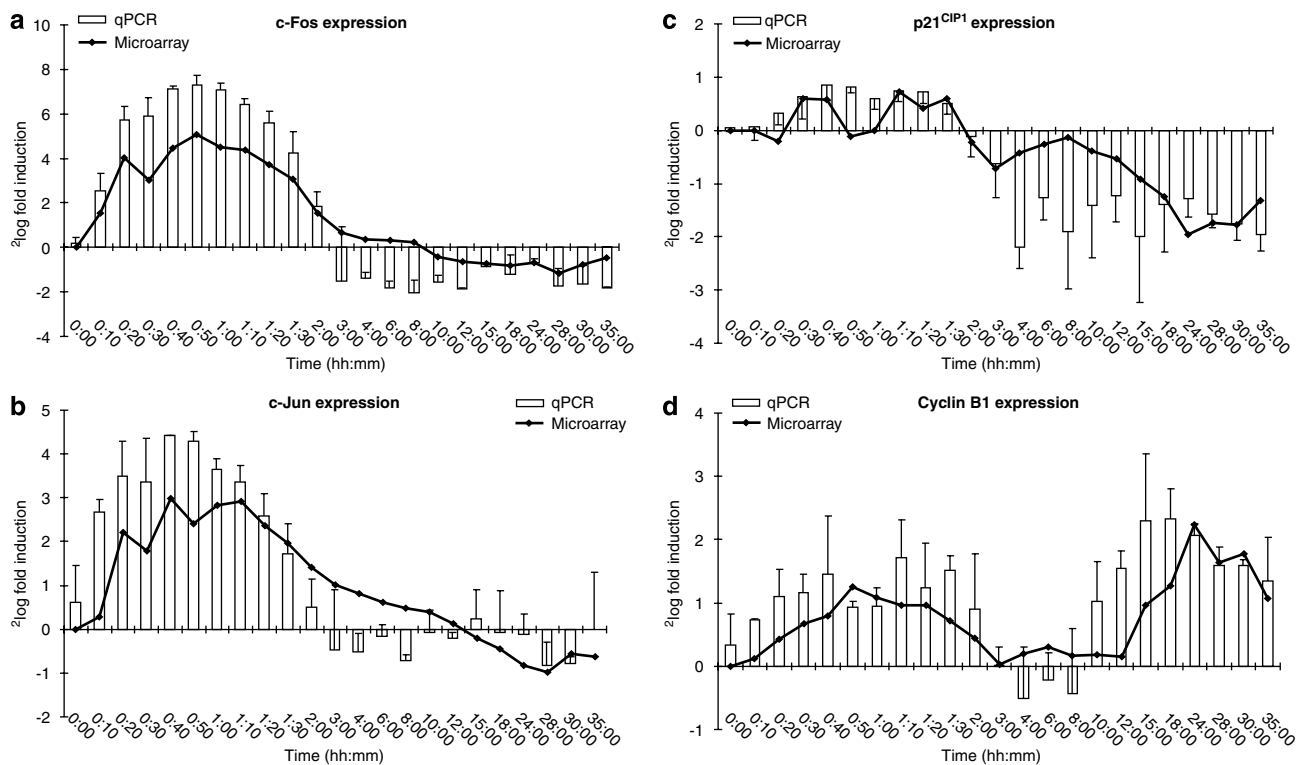


Figure 1 Microarray expression profiles of some key genes validated by quantitative PCR. (a–d) Relative amounts of c-Fos (a), c-Jun (b), p21^{CIP1} (c), cyclin B1 (d) mRNA levels as determined by microarray expression profiling (lines) and qPCR (white bars). Error bars represent s.d. between two independent experiments.

et al., 1999; Chang *et al.*, 2004). To understand which processes were occurring in cells released from G₂ arrest, we have used Genesis (Sturn *et al.*, 2002) to group genes in 10 different clusters using k-means clustering, each showing a specific expression profile over time. Figure 2a shows the profiles of the 10 clusters, a–j, starting with the cluster containing the earliest induced genes. The upper left graph shows the cell-cycle phase in which the majority of the cells were at the corresponding time point. The microarray complete data set has been submitted to ArrayExpress (accession E-NCMF-9).

To link the 10 clusters (Figure 2a) to biological processes we analysed their overlap with gene ontology (GO) categories. We first mapped all available probes to Entrez IDs. For the 8691 probes in the 10 clusters, 5915 probes could be associated to an Entrez ID. We considered all GO categories with at least five annotated genes present on the microarray (2217 sets). Using the hypergeometric distribution, we calculated a *P*-value indicating the significance of the overlap between a cluster and each GO category. We performed Benjamini and Hochberg (1995) multiple testing correction. Table 1 shows the GO categories that were significantly enriched in the respective clusters (*P* < 0.05).

The (immediate) early-induced gene clusters (a and b) showed enrichment for genes involved in growth factor signaling (chemokine and cytokine activity) (for example, genes involved in platelet-derived growth factor and epidermal growth factor signaling) and the RAS–mitogen-activated protein kinase (MAPK) pathway (mitogen-activated protein (MAP) kinase phosphatase activity, small GTPase-mediated signal transduction), which can be linked to apoptosis, cell growth and proliferation. The later induced gene clusters (c, d and e) mainly showed enrichment for metabolic pathways, such as amino acid and nucleotide biosynthesis and genes involved in rRNA, mRNA and tRNA processing. Cluster g showed enrichment for genes involved in the G₂/M checkpoint and processes in Sphase. Finally, clusters i and j, containing weakly and strongly downregulated genes, did not show enrichment for GO categories that we could link to the cell-cycle re-entry, although gene function analysis using Ingenuity (www.ingenuity.com) revealed enrichment for genes involved in cell-cycle arrest, such as p21^{CIP1} (data not shown). The lower right graph in Figure 2a summarizes how some of the main functions and genes were affected.

These results indicate that the strongest wave of transcriptional activity directly follows serum stimulation (within 1–2 h) and is associated with cellular proliferation, although cells remain arrested for 15 more hours. The later transcriptional response includes genes involved in cellular metabolism, followed by a repression of genes involved in cell-cycle arrest (such as p27^{KIP1} and p21^{CIP1}), which is consistent with the timing of cell-cycle re-entry.

Involvement of RAS and PI-3 kinase pathways

The RAS and PI-3 kinase pathways have previously been implicated in serum-induced cell-cycle re-entry of

G₁-arrested cells. Figures 2b and c show the expression profile of the strongest regulated genes in these pathways upon serum stimulation of G₂-arrested cells (upregulated or downregulated at least 2.2-fold at four time points or more). We confirmed these results for six of these genes by qPCR analysis and observed similar transcriptional responses (Figure 2d). Of the two proteins that are activated by the protein kinase B (PKB)/v-akt murine thymoma viral oncogene homolog (AKT)1 pathway, RHEB (Sarbasov *et al.*, 2005) and MDM2 (Feng *et al.*, 2004), the encoding genes were upregulated while *CDKN1A* (p21^{CIP1}) (Zhou *et al.*, 2001) and *TSC2* (Hay, 2005), whose gene products are inactivated by PKB/AKT, were downregulated. Furthermore, an inhibitor of PKB kinase activity, *GAB1*, was downregulated (Fan *et al.*, 2001). These observations are consistent with serum-induced activation of the PI-3 kinase pathway. In the RAS–MAPK pathway, *MYC*, *FOS* and *SRF* (serum-response factor) showed induction of expression indicative of activation of the RAS–MAPK pathway. However, *DUSP1*, 2, 4 and 6 (dual phosphatases 1, 2, 4 and 6), which are inhibitors of the RAS–MAPK pathway (Theodosiou and Ashworth, 2002), were also induced. Furthermore, two inhibitory subunits (PPP1R14B and C) of protein phosphatase 1 (PP1) were downregulated, suggesting that phosphatase activity that is involved in extracellular signal-regulated kinase (ERK) inhibition is induced in serum-stimulated cells. Finally, *MAPK3* (ERK1) was also transcriptionally downregulated. Thus, besides induction, the RAS–MAPK pathway is also suppressed by serum stimulation, possibly as the result of a negative feedback loop.

Taken together, these results strongly suggest that the core serum response of G₂-arrested cells is very similar to that of G₁-arrested cells.

Cell-cycle re-entry of G₂-arrested cells depends on RAS and PI-3 kinase signaling

From the microarray data, we found that several genes in the RAS and PI-3 kinase pathways were transcriptionally affected by serum stimulation, as has also been shown for wild-type human and wild-type mouse fibroblasts that were serum stimulated from G₁ (Iyer *et al.*, 1999; Chang *et al.*, 2004). However, serum stimulation does not only result in a transcriptional response, but also in activation of the RAS and PI-3 kinase pathways through post-translational modifications, such as phosphorylation (Campbell *et al.*, 1998). Therefore, we determined phosphorylation of ERK1/2, MAP-ERK kinase (MEK)1 and AKT in serum-stimulated TKO-BCL2 cells that were serum starved for 7 days. As a control, we determined AKT phosphorylation in serum-stimulated wild-type MEFs that had been serum starved for 48 h, showing phosphorylation at the earliest time point measured (30 min). Serum stimulation of TKO-BCL2 MEFs resulted in phosphorylation of ERK1, ERK2, AKT and MEK1 within 10 min after

serum stimulation (Figure 3a), similarly as described for wild-type MEFs (D'Abaco *et al.*, 2002), suggesting that the signaling cascades in cells recovering from a serum-starvation-induced G₁ or G₂ arrest were similar. We next used chemical inhibition to investigate further the significance of these pathways for cell-cycle re-entry

upon serum stimulation. G₂-arrested TKO-BCL2 MEFs were stimulated to enter the cell cycle by addition of 10% serum either in the absence or the presence of the MEK inhibitor PD98059, the PI-3 kinase inhibitor LY294002, or the CDK1/2 inhibitor Roscovitine. Mitotic entry normally occurs within 15h of serum

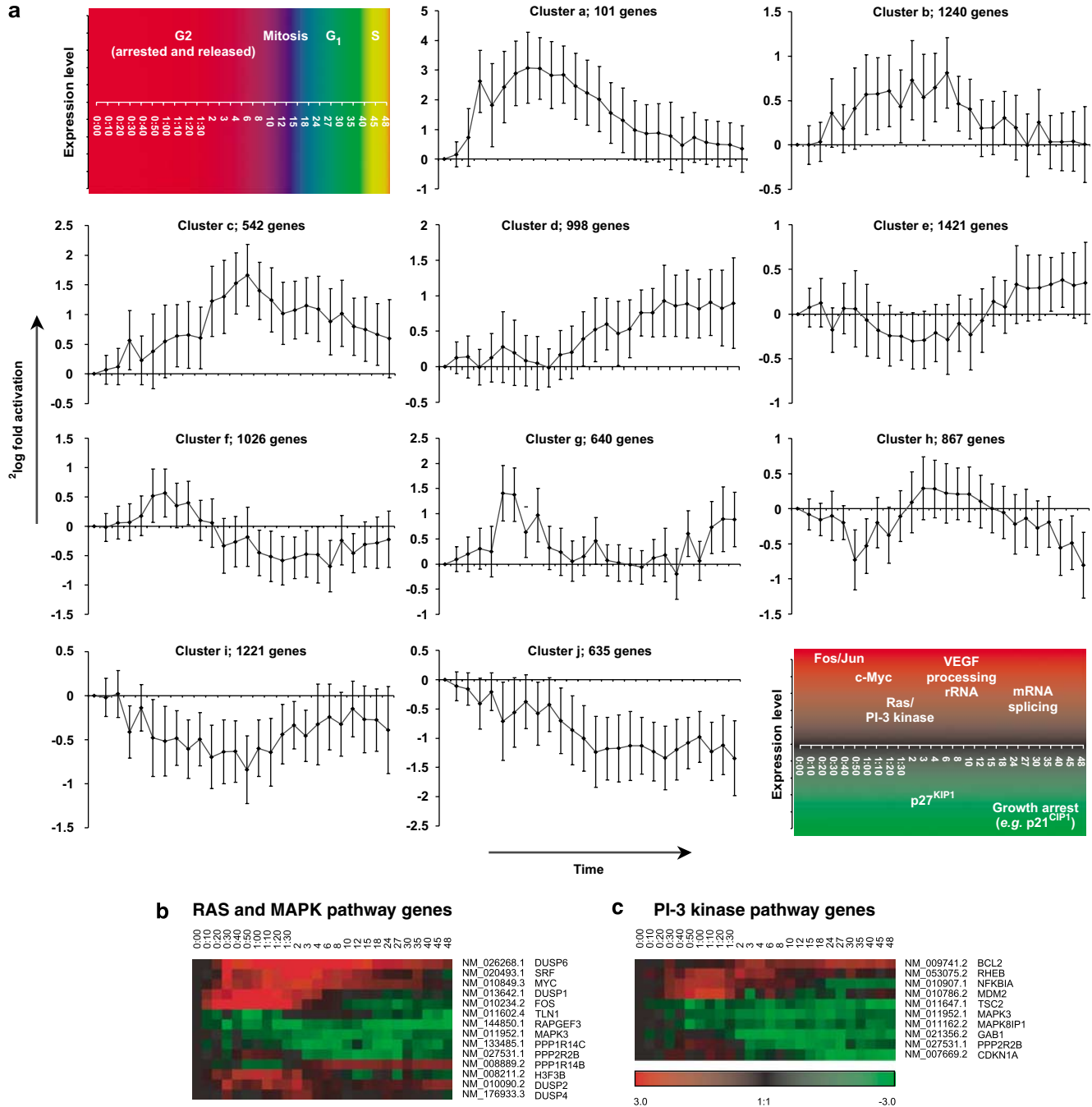


Figure 2 Expression profiles as a function of time after serum stimulation of G₂-arrested TKO-BCL2 cells (k-means clustering analysis as determined by Genesis). Error bars indicate s.d. of expression values within each cluster. Upper left diagram indicates the cell-cycle phase in which the cells were at different time points. Lower right diagram summarizes the up (red) or down (green) regulation of key molecular functions over time. **(b and c)** Expression profiles of genes associated with the RAS–MAPK pathway **(b)** and PI-3 kinase pathway **(c)** present in the expression profiling data set. **(d)** Relative amounts of DUSP6, PPP2R2B, c-MYC, TSC2, MAPK-3 and NFKBIA mRNA levels as determined by microarray expression profiling (lines) and qPCR (white bars). Error bars indicate the s.d. between two independent experiments. MAPK, mitogen-activated protein kinase; TKO, triple knockout.

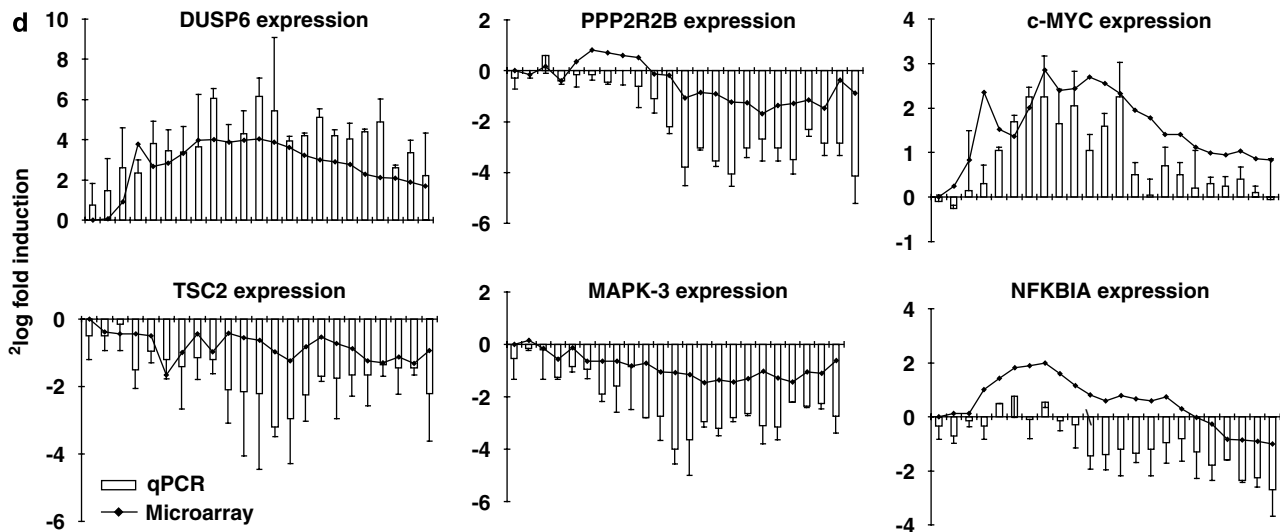


Figure 2 Continued.

stimulation but was completely blocked in the presence of Roscovitine (Figure 3b, compare black and dark gray bars). This is consistent with previous observations showing that cell-cycle re-entry is fully dependent on re-activation of cyclin A- and B-kinase activities (Nigg, 2001). Inhibition of MEK resulted in decreased and delayed entry into mitosis (Figure 3b, compare white and black bars). Additionally, we determined entry into G₁ as a measure for completion of mitosis. Inhibition of mitotic entry by PD98059 was accompanied by delayed appearance of G₁ cells (Figure 3c, compare upper and second row of histograms). Inhibition of the PI-3K pathway resulted in an even stronger delay of mitotic entry: only after 21–24 h the first mitotic events could be found (Figure 3b, light gray bars). The complete absence of G₁ cells suggests that LY294002-treated cells failed to exit mitosis or were severely delayed in mitotic progression (Figure 3c, third row of histograms). Combinational inactivation of the PI-3 kinase and RAS pathways prevented entry into mitosis of serum-stimulated TKO-BCL2 MEFs to the same extent as Roscovitine (Supplementary Figure 1).

Since recovery from G₂ arrest was accompanied by diminution of p21^{CIP1} and p27^{KIP1}, we have assessed the effects of inhibitor treatments on the levels of these CKIs. Figure 3d shows that without inhibitors, p27^{KIP1} level decreased within 12 h of serum induction, whereas p21^{CIP1} level decreased later on. PD98059 or Roscovitine treatment did not affect p27^{KIP1} or p21^{CIP1} degradation. However, inhibition of PI-3 kinase activity by LY294002 prevented the disappearance of p27^{KIP1}, but not of p21^{CIP1}.

Together, these results indicate that cell-cycle re-entry of G₂-arrested cells depends on the RAS and PI-3 kinase pathways. However, while the PI-3 kinase pathway is required for downregulation of p27^{KIP1} levels, the RAS pathway seems to act downstream of the CKIs, perhaps more directly on cyclin A- and B-associated kinase activity.

Oncogenic events that disrupt the G₂-restriction point

The G₂-restriction point may function as an emergency brake in cells in which the G₁-restriction point is compromised; a common event in human cancer (Hanahan and Weinberg, 2000). As this emergency brake might constrain proliferation of premalignant cells *in vivo*, we were interested whether oncogenic events other than p53 loss might override the G₂-restriction point. Given the strong induction of c-MYC upon serum stimulation (Supplementary dataset 1) and the dependence of cell-cycle re-entry on the RAS pathway (Figure 2b), we wondered whether oncogenic events such as c-MYC overexpression or RAS^{V12} mutation could inactivate the G₂-restriction point. For this purpose, we serum-starved TKO-BCL2 MEFs that were infected with retroviral vectors encoding oncogenic RAS (pbp-RAS^{V12}) or c-MYC (pbp-c-MYC) and compared their responses to control-infected (pbp) TKO-BCL2 MEFs. Whereas the vast majority of the control-infected cells accumulated in G₂ upon 7 days of serum starvation (Figure 4a, black bars), both RAS^{V12}- and c-MYC-infected cells were compromised in their ability to arrest in G₂ (Figure 4a, white and gray bars). Growth curves indicate that pbp-RAS^{V12}-infected cells indeed continued to proliferate in the absence of serum similar to TKO-p53RNAi MEFs (Figure 4b; Fojjer *et al.*, 2005). Surprisingly, however, numbers of pbp-c-MYC-infected cells did not increase (Figure 4b). We therefore compared the cell-cycle profiles of serum-starved mock-, c-MYC- or RAS^{V12}-infected TKO-BCL2 cells and measured the level of 5-bromo-2-deoxyuridine (BrdU) incorporation. Figure 4c–e shows that although BrdU incorporation was strongly decreased in all three cell lines, RAS^{V12} and c-MYC infected cells both maintained a high level of G₁ cells (Figures 4d and e). However, in contrast to RAS^{V12}-infected cells, we found that c-MYC cells, despite the presence of BCL2, were highly prone to apoptosis when serum starved (Figure 4f). These data suggest that that both c-MYC

Table 1 Enriched GO categories in different clusters

GO ids	GO description	Raw P-values	Corrected P-values (Benjamini/Hochberg)	No. of genes in GO category	No. of genes overlap- ping with cluster
<i>Cluster a, 88 out of 101 genes^a</i>					
GO:0017017	MAP kinase phosphatase activity	7.15E-08	0.000158	10	4
GO:0008009	Chemokine activity	1.59E-07	0.000176	29	5
GO:0005125	Cytokine activity	2.57E-07	0.000190	146	8
GO:0008201	Heparin binding	2E-06	0.001108	85	6
GO:0005576	Extracellular region	8.56E-06	0.003795	483	11
GO:0006935	Chemotaxis	3.04E-05	0.011200	82	5
GO:0006954	Inflammatory response	3.54E-05	0.011200	140	6
<i>Cluster b, 946 of 1240 genes^a</i>					
GO:0005634	Nucleus	1.09E-10	2.41E-07	3912	264
GO:0003723	RNA binding	1.66E-06	0.001307	611	56
GO:0005515	Protein binding	1.77E-06	0.001307	4800	288
GO:0003743	Translation initiation factor activity	2.72E-05	0.014387	82	14
GO:0015031	Protein transport	3.24E-05	0.014387	458	42
GO:0045766	Positive regulation of angiogenesis	4.79E-05	0.015390	10	5
GO:0006888	ER to Golgi vesicle-mediated transport	5.91E-05	0.015390	77	13
GO:0005681	Spliceosome	6.02E-05	0.015390	134	18
GO:0007028	Cytoplasm organization and biogenesis	6.86E-05	0.015390	6	4
GO:0008380	RNA splicing	6.94E-05	0.015390	173	21
GO:0006397	mRNA processing	9.77E-05	0.019693	217	24
GO:0031202	RNA splicing factor activity, <i>trans</i> esterification mechanism	0.000124	0.022034	18	6
GO:0006916	Antiapoptosis	0.000134	0.022034	106	15
GO:0000245	Spliceosome assembly	0.000139	0.022034	12	5
GO:0051920	Peroxiredoxin activity	0.000154	0.022767	7	4
GO:0007264	Small GTPase mediated signal transduction	0.000223	0.030869	243	25
GO:0000074	Regulation of progression through cell cycle	0.000309	0.040023	234	24
GO:0006376	mRNA splice site selection	0.000325	0.040023	14	5
GO:0000166	Nucleotide binding	0.000354	0.041321	1952	124
GO:0030529	Ribonucleoprotein complex	0.000421	0.046713	239	24
<i>Cluster c, 377 of 542 genes^a</i>					
GO:0005730	Nucleolus	3.5E-15	7.76E-12	115	21
GO:0006364	rRNA processing	8.14E-11	9.03E-08	49	12
GO:0000178	Exosome (RNase complex)	6.53E-07	0.000483	18	6
GO:0003723	RNA binding	3.97E-05	0.021985	611	27
GO:0005759	Mitochondrial matrix	0.000106	0.047130	14	4
<i>Cluster d, 515 of 998 genes</i>					
GO:0005739	Mitochondrion	1.9E-18	4.22E-15	836	70
GO:0005763	Mitochondrial small ribosomal subunit	2.98E-12	3.19E-09	13	9
GO:0030529	Ribonucleoprotein complex	4.32E-12	3.19E-09	239	29
GO:0003735	Structural constituent of ribosome	5.86E-12	3.25E-09	150	23
GO:0006412	Translation	6.8E-11	3.02E-08	285	30
GO:0006457	Protein folding	3.31E-10	1.22E-07	215	25
GO:0043234	Protein complex	2.96E-08	9.38E-06	98	15
GO:0005840	Ribosome	4.01E-08	1.11E-05	130	17
GO:0005829	Cytosol	1.44E-06	0.000356	328	25
GO:0003755	Peptidyl-prolyl <i>cis-trans</i> isomerase activity	1.82E-06	0.000403	34	8
GO:0005839	Proteasome core complex (sensu Eukaryota)	2.72E-06	0.000549	17	6
GO:0004298	Threonine endopeptidase activity	3.99E-06	0.000738	18	6
GO:0005743	Mitochondrial inner membrane	7.03E-06	0.001198	248	20
GO:0009306	Protein secretion	1.19E-05	0.001787	13	5
GO:0016853	Isomerase activity	1.21E-05	0.001787	137	14
GO:0004175	Endopeptidase activity	1.7E-05	0.002356	33	7
GO:0005762	Mitochondrial large ribosomal subunit	1.95E-05	0.002539	23	6
GO:0005761	Mitochondrial ribosome	3.8E-05	0.004678	16	5
GO:0008380	RNA splicing	4.24E-05	0.004948	173	15
GO:0006397	mRNA processing	4.89E-05	0.005419	217	17
GO:0006164	Purine nucleotide biosynthetic process	7.14E-05	0.007537	18	5
GO:0000398	Nuclear mRNA splicing, via spliceosome	8.04E-05	0.008098	29	6
GO:0045454	Cell redox homeostasis	0.000126	0.012177	59	8
GO:0015450	Protein translocase activity	0.000181	0.016731	12	4
GO:0005788	Endoplasmic reticulum lumen	0.000256	0.021856	13	4
GO:0006790	Sulfur-metabolic process	0.000256	0.021856	13	4
GO:0006511	Ubiquitin-dependent protein catabolic process	0.000413	0.033881	126	11
<i>Cluster e, 822 of 1421 genes^a</i>					
GO:0005739	Mitochondrion	1.5E-10	2.79E-07	836	75
GO:0030529	Ribonucleoprotein complex	2.52E-10	2.79E-07	239	34
GO:0006412	Translation	8.07E-07	0.000596	285	31
GO:0003735	Structural constituent of ribosome	1.27E-05	0.007033	150	19

Table 1 (continued)

GO ids	GO description	Raw P-values	Corrected P-values (Benjamini/Hochberg)	No. of genes in GO category	No. of genes overlap- ping with cluster
GO:0005840	Ribosome	2.36E-05	0.010471	130	17
GO:0016491	Oxidoreductase activity	2.89E-05	0.010673	756	55
GO:0003954	NADH dehydrogenase activity	3.39E-05	0.010737	32	8
GO:0008137	NADH dehydrogenase (ubiquinone) activity	5.44E-05	0.015079	34	8
GO:0006139	Nucleobase, nucleoside, nucleotide and nucleic acid metabolic process	0.000148	0.036402	49	9
GO:0046034	ATP-metabolic process	0.000172	0.038215	8	4
<i>Cluster f, 697 of 1026 genes^a</i>					
GO:0005515	Protein binding	3.66E-07	0.000812	4800	224
GO:0005764	Lysosome	8.71E-06	0.009657	127	16
<i>Cluster g, 429 of 640 genes^a</i>					
GO:0005634	Nucleus	1.21E-20	2.69E-17	3912	166
GO:0007049	Cell cycle	4.05E-10	4.45E-07	437	33
GO:0051276	Chromosome organization and biogenesis	6.02E-10	4.45E-07	11	7
GO:0005694	Chromosome	1.87E-09	1.04E-06	111	16
GO:0006974	Response to DNA damage stimulus	1.56E-08	6.90E-06	183	19
GO:0003676	Nucleic acid binding	2.1E-08	7.47E-06	1313	60
GO:0006259	DNA-metabolic process	2.36E-08	7.47E-06	44	10
GO:0006281	DNA repair	2.87E-08	7.96E-06	190	19
GO:0000166	Nucleotide binding	3.96E-07	9.51E-05	1952	75
GO:0005515	Protein binding	4.29E-07	9.51E-05	4800	148
GO:0000776	Kinetochore	4.96E-07	9.99E-05	24	7
GO:0007059	Chromosome segregation	5.86E-07	0.000108	35	8
GO:0051301	Cell division	8.64E-07	0.000147	236	19
GO:0003723	RNA binding	1.21E-06	0.000192	611	33
GO:0046982	Protein heterodimerization activity	1.7E-06	0.000251	101	12
GO:0007067	mitosis	2.28E-06	0.000317	142	14
GO:0008026	ATP-dependent helicase activity	6.12E-06	0.000799	114	12
GO:0006260	DNA replication	8.76E-06	0.001079	118	12
GO:0004386	Helicase activity	1.85E-05	0.002154	148	13
GO:0003779	Actin binding	3.65E-05	0.004150	333	20
GO:0000922	spindle pole	3.99E-05	0.004209	19	5
GO:0006397	mRNA processing	7.24E-05	0.007291	217	15
GO:0005524	ATP binding	0.000163	0.015513	1705	59
GO:0005737	Cytoplasm	0.000168	0.015513	1595	56
GO:0051082	Unfolded-protein binding	0.000199	0.017653	75	8
GO:0051010	Microtubule plus-end binding	0.00032	0.027027	7	3
GO:0007001	Chromosome organization and biogenesis (sensu Eukaryota)	0.00033	0.027027	44	6
GO:0016363	Nuclear matrix	0.000341	0.027027	29	5
GO:0008380	RNA splicing	0.000363	0.027027	173	12
GO:0016605	PML body	0.000395	0.029198	17	4
<i>Cluster h, 699 of 867 genes^a</i>					
GO:0005634	Nucleus	5.38E-08	0.000119	3912	194
GO:0006397	mRNA processing	7.82E-06	0.006061	217	22
GO:0005515	Protein binding	8.2E-06	0.006061	4800	217
GO:0003723	RNA binding	2.44E-05	0.013529	611	42
GO:0003677	DNA binding	5.63E-05	0.024978	1905	98
GO:0005681	Spliceosome	6.93E-05	0.025609	134	15
GO:0008380	RNA splicing	0.000121	0.038337	173	17
<i>Cluster i, 838 of 1221 genes^a</i>					
None with corrected $P < 0.05$					
<i>Cluster j, 504 of 635 genes^a</i>					
GO:0005578	Proteinaceous extracellular matrix	5.57E-08	0.000124	323	27
GO:0005515	Protein binding	1.46E-06	0.001622	4800	167
GO:0005615	Extracellular space	4.89E-06	0.003617	2085	85
GO:0008201	Heparin binding	9.09E-06	0.005039	85	11
GO:0016504	Protease activator activity	1.3E-05	0.005778	7	4
GO:0004364	Glutathione transferase activity	1.72E-05	0.006367	23	6
GO:0005604	Basement membrane	2.82E-05	0.008932	79	10
GO:0009888	Tissue development	3.43E-05	0.009493	16	5
GO:0005764	Lysosome	8.81E-05	0.021697	127	12
GO:0007155	Cell adhesion	0.000104	0.023075	564	30
GO:0008203	Cholesterol-metabolic process	0.000161	0.032382	47	7

Abbreviations: GO, gene ontology; MAP, mitogen-activated protein; ER, endoplasmic reticulum; NADH, nicotinamide adenine dinucleotide. *x out of y genes: indicates that x genes of the cluster containing y genes could be associated to an Entrez ID.

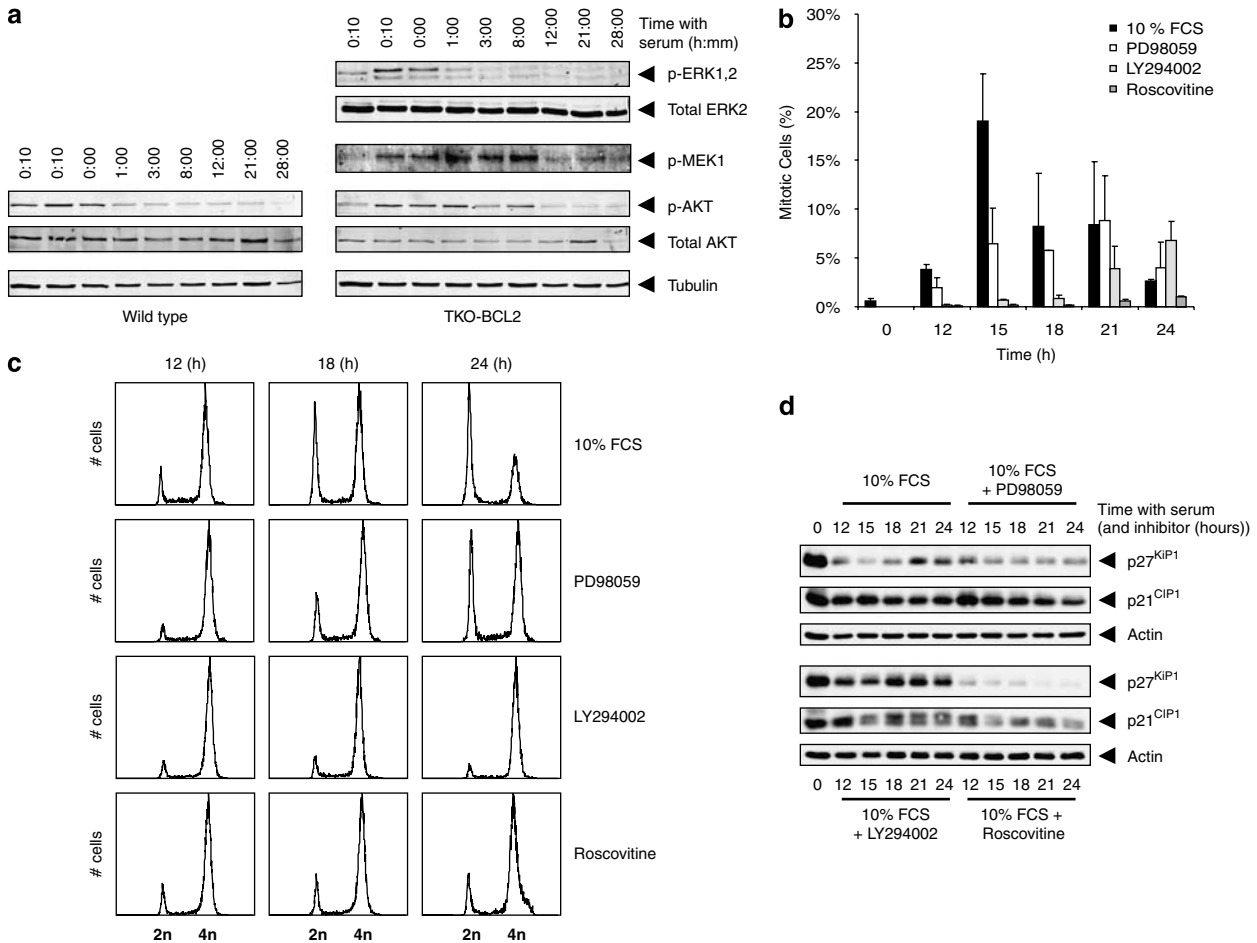


Figure 3 Cell-cycle re-entry from serum-starvation-induced G₂ arrest depends on RAS and PI-3 kinase signaling. (a) Western blots showing phosphorylated AKT, MEK1, ERK1 and ERK2 and total AKT and ERK2 of serum-stimulated TKO-BCL2 MEFs (right panels) and phosphorylated and total AKT in serum-stimulated wild-type MEFs (left panels) for the indicated times. Tubulin functions as a loading control for total protein. (b) Mitotic entry as determined by MPM2 positivity on FACS of TKO-BCL2 MEFs that were serum stimulated in the absence (black bars) or in the presence of the MEK inhibitor PD98059 (white bars), the PI-3 kinase inhibitor LY294002 (gray bars) or the CDK1/2 inhibitor Roscovitine (dark-gray bars). Error bars show s.d. of two independent experiments. (c) Histograms showing cell-cycle distributions of serum-stimulated TKO-BCL2 MEFs in the absence (upper row) or in the presence of PD98059 (second row), LY294002 (third row) or Roscovitine (fourth row) as determined by FACS analyses of propidium iodide-stained cells. (d) Western blots showing p21^{CIP1} and p27^{KIP1} levels in serum-stimulated TKO-BCL2 cells in the presence or absence of PD98059, LY294002 or Roscovitine at several time points. The level of actin functions as a loading control. FCS, fetal calf serum; MEFs, mouse embryonic fibroblasts; TKO, triple knockout.

and RAS^{V12} were capable of alleviating the serum-starvation-induced G₂ arrest, allowing progression through the cell cycle in the absence of mitogens. Whereas RAS^{V12}-expressing cells accumulated, the majority of c-MYC-expressing cells underwent apoptosis.

To investigate further the effect of c-MYC over-expression on the G₂-restriction point, we compared the stability of p21^{CIP1} and p27^{KIP1} in mock-, p53RNAi- and c-MYC-infected TKO-BCL2 cells by using the translation inhibitor cycloheximide and the proteasome inhibitor MG-132. Under high-serum conditions, p21^{CIP1} and p27^{KIP1} are known to be unstable due to high-cyclin-dependent kinase activity (Morisaki *et al.*, 1997; Zhu *et al.*, 2005). Indeed, both p21^{CIP1} and p27^{KIP1} were subjected to protein degradation under high-serum conditions in the three cell types, as cycloheximide

treatment resulted in reduced protein levels (Figure 4g, compare lanes 1 and 2, lanes 4 and 5 and lanes 7 and 8). Correspondingly, both CKI levels increased upon MG-132 treatment, suggesting protein synthesis during the treatment period (Figure 4g, compare lanes 1 and 3, lanes 4 and 6 and lanes 7 and 9).

Serum deprivation resulted in stabilization of p21^{CIP1} and p27^{KIP1} in TKO-BCL2 MEFs, as cycloheximide treatment no longer reduce the CKI levels (Figure 4f, compare lanes 10 and 11). MG-132 treatment led to an induction of p21^{CIP1} levels, suggesting protein synthesis (Figure 4f, lane 12). In TKO-p53RNAi MEFs, p21^{CIP1} protein was practically absent and appeared to decrease upon cycloheximide treatment, suggesting it was highly unstable in these cells (Figure 4f, lanes 13 and 14). Also p27^{KIP1} was still subjected to degradation (Figure 4f,

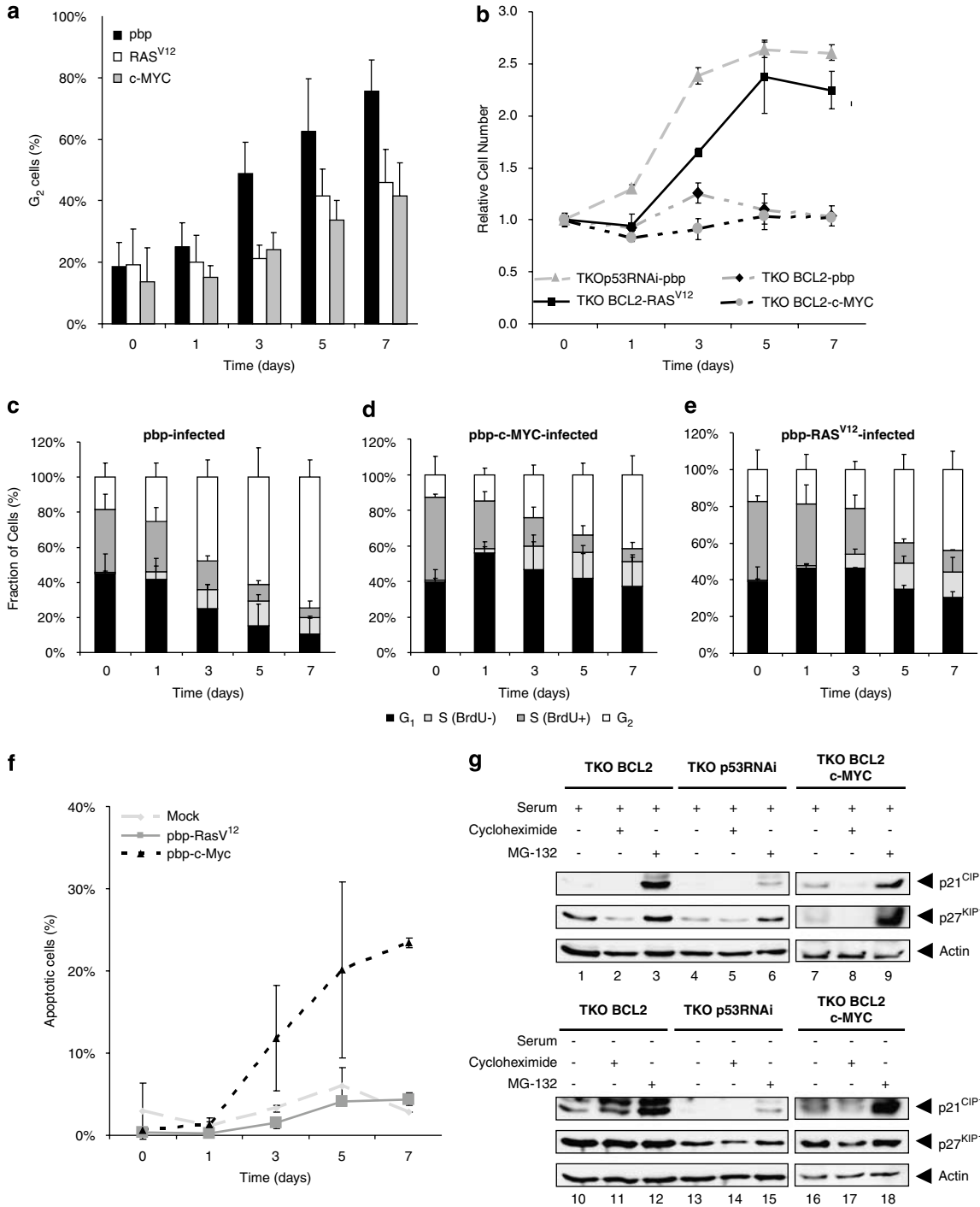


Figure 4 Oncogenic events that alleviate the G₂-restriction point. **(a)** Accumulation in G₂ of control-transduced (black bars), RAS^{V12}-transduced (white bars) or c-MYC-transduced TKO-BCL2 cells in G₂ upon serum deprivation. Error bars indicate s.d. of at least three independent experiments. **(b)** Growth curves of control-transduced (diamonds), c-MYC-transduced (circles) and RAS^{V12}-transduced (squares) TKO-BCL2 MEFs and control-transduced TKO-p53RNAi MEFs (triangles). Error bars indicate s.d. of three experiments. **(c–e)** Cell-cycle distribution of mitogen-deprived control-transduced **(c)**, c-MYC-transduced **(d)** or RAS^{V12}-transduced **(e)** TKO-BCL2 MEFs. Sphase was determined by BrdU incorporation. BrdU- indicates cells that were negative for BrdU staining with a DNA content in between G₁ and G₂. Error bars show s.d. of at least three independent experiments. **(f)** Apoptotic fraction of serum-starved mock- (light gray line), RAS^{V12} (dark gray line) or c-MYC-infected TKO-BCL2 MEFs as determined by flow cytometry (sub-G₁ fraction). Error bars indicate the s.d. between the two experiments. **(g)** Western blots showing p21^{CIP1} and p27^{KIP1} levels in TKO-BCL2, TKO-p53RNAi and c-MYC-transduced TKO-BCL2 MEFs under high-serum conditions and under serum-free conditions (3 days), treated with cycloheximide or MG-132 to determine protein stability. The level of actin functions as a loading control. MEFs, mouse embryonic fibroblasts; RNAi, RNA interference; TKO, triple knockout.

lanes 13–15). C-MYC infected cells clearly behaved like TKO-p53RNAi cells: both CKIs were subjected to degradation (Figure 4f, lanes 16–18). Thus, serum deprivation in TKO-BCL2 cells resulted in stabilization of p21^{CIP1} and p27^{KIP1}, which was dependent on p53 and could be prevented by c-MYC. We therefore envisage that c-MYC expression in TKO cells alleviated mitogen starvation-induced G₂ arrest by preventing stabilization of p21^{CIP1} and p27^{KIP1}.

Collectively, these results indicate that oncogenic events like mutation of RAS to its oncogenic variant RAS^{V12}, amplification of c-MYC or loss of p53 can result in disruption of the G₂-restriction point, and may therefore be important alterations in transformation of pocket protein-deficient cells.

Discussion

Mitogen-independent growth is a hallmark of cancer cells (Hanahan and Weinberg, 2000). Understanding the mechanisms that lead to mitogen-independent growth are therefore of crucial importance to design new therapies that defeat cancer. Pocket proteins are essential for the integrity of the G₁-restriction point that forces cells to arrest in the absence of growth factors (Dannenberg *et al.*, 2000; Sage *et al.*, 2000; Foijer *et al.*, 2005). However, examination of cells suffering from (partial) absence of pocket protein activity has uncovered another restriction point that arrests cells in G₂ (Foijer *et al.*, 2005; Foijer and te Riele, 2006b). The serum-starvation-induced G₂ arrest is completely reversible by mitogen re-addition resulting in synchronous mitotic entry after approximately 15 h. We have made a survey of the molecular (transcriptionally regulated) pathways that are involved in cell-cycle re-entry from G₂ arrest by profiling the transcriptome of serum-stimulated TKO-BCL2 MEFs in time. Mitogen stimulation of G₂-arrested TKO-BCL2 MEFs resulted in transcriptional activation of many well-known serum-inducible factors such as c-Fos, c-Jun, serum- and glucocorticoid-inducible kinase (SGK), serum-response factor and many others. The immediate response was followed by upregulation or downregulation of genes involved in the RAS and PI-3 kinase pathways and cell-cycle genes such as *CDK1* (*CDC2*) and *Cyclin B1*, likely as a consequence of c-MYC activation (Guo *et al.*, 2000; Oster *et al.*, 2002). After this initial response, cells re-initiated their metabolic processes as was evidenced by induction of genes involved in RNA processing, nucleotide synthesis and amino-acid metabolism. Cluster g formed an exception, since this cluster contained genes that were upregulated 1 h after serum stimulation and again at 40 h, when cells entered S phase. Indeed, this cluster contained several genes that are normally upregulated in S phase, but also genes that are involved in DNA damage response. We are currently verifying this part of the serum response and investigating whether the early peaking of DNA damage response genes is caused by DNA damage that can only be sensed in the presence of mitogens, or is a consequence of, for instance, early E2F

activation. Finally, clusters i and j showed (late) transcriptional repression of inhibitors of CDK1-kinase activity from 6 to 10 h on after serum stimulation (Figure 2a). This may offer an explanation for the late re-activation of cyclin B1-CDK1 kinase activity and mitotic entry despite the early induction (within 1–2 h after serum stimulation) of many cell-cycle-promoting genes. Overall, the serum responses of G₁-arrested and G₂-arrested cells are highly similar, suggesting that the mechanisms underlying the G₁- and G₂-restriction points are largely the same.

Pathways involved in G₂ arrest

An important limitation of microarray expression profiling is that it excludes post-translational modifications of proteins, which make up an important part of the serum response. For example, mitogen binding to receptors results in activation of RAS, promoting phosphorylation of the MAPK kinases MEK1 and 2 via binding to RAF-1 kinase. Activated RAS can also activate PI-3 kinase by means of direct association (Campbell *et al.*, 1998). To include this part of the serum response in our analysis, we used chemical inhibitors to block the RAS and PI-3 kinase pathways in G₂-arrested cells during serum re-stimulation. These experiments unequivocally showed that serum-starved TKO-BCL2 cells need both RAS and PI-3 kinase signaling for cell-cycle re-entry. One may argue that the requirement for the RAS pathway is a direct consequence of activation of PI-3 kinase by RAS (Campbell *et al.*, 1998). However, PD98059 inhibits the RAS pathway by inhibiting MEK kinase, downstream of RAS, thus leaving the PI-3 kinase pathway unaffected (Dudley *et al.*, 1995). Moreover, unlike inhibition of the PI-3 kinase pathway, inhibition of the RAS–MEK pathway did not affect CKI degradation. In addition, we found that combinational inactivation of RAS and PI-3 kinase resulted in an exaggerated phenotype. This suggests that RAS and PI-3 kinase function in independent pathways that are both crucial for cell-cycle re-entry of serum-starved G₂-arrested cells. Thus, also in this respect serum-starved G₂-arrested TKO cells resemble serum-starved G₁-arrested wild-type cells and may therefore similarly be considered as G₀ cells.

Consistent with the chemical inhibitor experiments, we showed that overexpression of RAS^{V12} can prevent pocket protein-deficient cells from arresting in G₂ in the absence of mitogens. In addition, we showed that c-MYC overexpression led to destabilization of p21^{CIP1} and p27^{KIP1}, similar to suppression of p53 by RNAi. However, in contrast to p53RNAi- or RAS^{V12}-expressing cells, c-MYC overexpressing cells did not accumulate under serum-deprived conditions, which we could attribute to apoptosis, despite the presence of BCL2. Presumably, elevated E2F activity through pocket protein ablation combined with c-MYC overexpression generates an apoptotic response that cannot be counteracted by BCL2.

Oncogenic transformation is a multistep process (Hanahan and Weinberg, 2000) requiring the breaching

of several barriers that protect normal cells against unconstrained proliferation. One of these barriers is manifested by growth arrest in the absence of mitogens. We found that mitogenic signaling is not only required for passage through G₁, but also for passage through G₂. We found that the latter can be relieved by oncogenic events such as loss of p53, expression of c-MYC or mutational activation of RAS. This may provide a novel rationale for the cooperation of these events and loss or oncogene-mediated inactivation of the *RB* gene family in development of cancer.

Materials and methods

Cell culture

MEFs were derived from chimeric embryos and cultured in Glasgow minimal essential medium (GMEM) (Invitrogen–Gibco, Carlsbad, CA, USA), supplemented with 10% fetal calf serum, 1 mM nonessential amino acids (Invitrogen–Gibco), 1 mM sodium pyruvate (Invitrogen–Gibco), 100 µg/ml penicillin, 100 µg/ml streptomycin (Invitrogen–Gibco) and 0.1 mM β-mercaptoethanol (Merck, Whitehouse Station, NJ, USA) as described previously (Foijer *et al.*, 2005). For serum-starvation experiments, approximately 4 × 10⁵ cells were seeded on 10 cm dishes (BD Falcon, Franklin Lakes, NJ, USA) and cultured under serum-free conditions up to 7 days. For serum-stimulation experiments, serum-free medium was replaced by complete medium. Growth curves were performed as described previously (Dannenbergh *et al.*, 2000). Inhibitors (Roscovitine, PD98059 and LY294002) were obtained from Biomol (Plymouth Meeting, PA, USA) and dissolved in dimethylsulfoxide. We used 50 µM based on Meijer *et al.* (1997) (for Roscovitine), Valledor *et al.* (2000) (for PD98059) and Knight *et al.* (2006) (for LY294002). Furthermore, we found that 20 µM of LY294002 resulted in a shorter delay of cell-cycle re-entry upon serum stimulation (not shown). Inhibitor containing medium was refreshed for time points exceeding 12 h. For stability experiments, cells were treated with 50 µg/ml cycloheximide or 5 µM MG-132 (Sigma-Aldrich, St Louis, MO, USA) for 2 h.

RNA isolation, quantitative PCR and microarray expression profiling

For quantitative PCR and microarray expression profiling, cells were harvested in RNazol B (Campro Scientific, Berlin, Germany) and RNA was isolated. For qPCR, 1 µg of total RNA was used for a reverse transcriptase reaction (Superscript II, Invitrogen, Carlsbad, CA, USA). The resulting cDNA was used as a template for qPCR in the presence of SYBR-green (Applied Biosystems, Foster City, CA, USA) to label the product. Relative amounts of cDNA were compared to actin as a reference for total cDNA and subsequently normalized for the amount of cDNA in the reference sample. The qPCR-primers used were the following. JUN FW: 5'-GAAAACCTT GAAAGCGCAAAA-3', RV: 5'-CACCTGTTCCCTGAGCA TGTT-3', FOS: FW: 5'-CCAAGCGGAGACAGATCAACT-3', RV: 5'-TCTCTTTTACAGCAGATTGGCAATC-3', cyclin B1: FW: 5'-TGTGTCCATTATTGATCGGTTCA-3', RV: 5'-CA CCGACCAGCTGTAGCATCT-3', p21^{CIP1}: FW: 5'-CCCGA GAACGGTGGAACTT-3', RV: 5'-CCAGACGAAGTTGC CCTCC-3' DUSP6 FW: 5'-TTCCTACTCTCGGATCATCG GA-3' RV: 5'-ACCAGGACACCCATGTTTTT-3', c-MYC FW: 5'-TGGTGAACGAGACAGCTTCTATCT-3', RV: 5'-CTGA GAAACCGCTCCACATAC-3', PPP2R2B: FW: 5'-CCTCA

ACAAAACGCAGCTTAC-3', RV: 5'-GTTGTAGCCTTCT GGCCTCTT-3', MAPK3: FW: 5'-CTGGCTTTCTGACGG AGTATG-3', RV: 5'-CAGACCAGATGTCGATGGATT-3', TSC2: FW: 5'-GACATGGGATATTCTGCTGGA-3', RV: 5'-CATGGACGATGGTCTTGTAGTT-3', NFKBIA: FW: 5'-GT GTAGCAGTCTTGACGCAGA-3', RV: 5'-TGGATAGAG GCTAGGTGCAGA-3'. Microarray expression profiling protocols can be found online on <http://microarray.nki.nl>. Briefly, total RNA samples were DNase-treated (Qiagen, Valencia, CA, USA) followed by a reverse transcriptase reaction (Superscript II, Invitrogen) in the presence of an oligo-T7 primer. Double-stranded cDNA was generated in a second-strand reaction, which was used for RNA synthesis (T7 Megascript, Ambion, Applied Biosystems, Austin, TX, USA) for hybridization. RNA was labeled by binding the N7 position of guanine using Universal Linkage System (ULS, Kreatech Biotechnology, LG Amsterdam, The Netherlands) to Cy 5 or Cy 3 dyes (Amersham Biosciences, Piscataway, NJ, USA). The resulting probe was hybridized to 32K NKI mouse oligo-microarrays according to the Netherlands Cancer Institute's Central Microarray Facility standard procedures. Arrays were scanned (Agilent Technologies, Santa Clara, CA, USA) and analysed using Imagen Software (Biodiscovery, El Segundo, CA, USA). Normalization and dye swap comparisons were performed using the Central Microarray Facility Database software. Expression values were exported to Microsoft Excel and clustered using Genesis software (Sturn *et al.*, 2002). Gene lists were analysed using a Matlab application (code available upon request) or uploaded to Ingenuity (www.ingenuity.com).

Constructs, transfection and retroviral infections

Generation of TKO-BCL2 or TKO-p53RNAi MEFs were described previously (Foijer *et al.*, 2005). Retroviral vectors were obtained from Drs. Bruno Amati (pbp-c-MYC) (Alevizopoulos *et al.*, 1997) and Daniel Peeper (pbp-RAS^{V12}) (Peeper *et al.*, 2001). Ecotropic retroviruses were produced in Phoenix cells through calcium phosphate co-precipitation of the retroviral vectors. MEFs were infected in triplicate with 0.45 µm filtered retroviral supernatants in the presence of 4 µg/ml polybrene and allowed to recover from the infection for 5 days before experiments.

FACS analysis

To determine S-phase cells, cells were incubated with 10 mM 5-bromodeoxyuridine for 1 h and subsequently fixed in 70% ethanol in phosphate-buffered saline at 4°C. Cells were stained with mouse anti-BrdU as described previously (Brugarolas *et al.*, 1998) or stained for MPM2 positivity (Smits *et al.*, 2000a). Cell-cycle distribution was analysed by FACS using 'Cell Quest' software (BD Biosciences, Franklin Lakes, NJ, USA) and 'FACS Express' software (De Novo Software).

Immunoblots and antibodies

Cells were harvested and subsequently lysed for 30 min in cell lysis buffer (ELB) (150 mM NaCl; 50 mM 4-(2-hydroxyethyl)-1-piperazineethanesulfonic acid pH 7.5; 5 mM ethylenediaminetetraacetic acid; 0.1% NP-40) containing protease inhibitors (Complete; Roche, Basel, Switzerland) and phosphatase inhibitors (5 mM NaF, 0.5 mM sodium vanadate and 20 mM β-glycerolphosphate). Protein concentrations were determined using the Bradford assay (BioRad, Life Science Research, Hercules, CA, USA). The antibodies used were mouse anti-p21 (F5) mouse anti-ERK2 (K23), goat anti-actin (I19) (Santa Cruz, Santa Cruz, CA, USA), mouse anti-p27 (BD Transduction Laboratories, Franklin Lakes, NJ, USA), mouse anti-AKT (5G3), rabbit anti-phospho-AKT^{Ser473} (193H12), rabbit

anti-phospho-ERK1^{Thr202}, 2^{Tyr204} (197G2), rabbit anti-phospho-MEK1^{Ser221}, (166F8) (Cell Signaling Technology, Danvers, MA, USA) mouse anti-tubulin (Abcam, Cambridge, MA, USA) MPM2 (Upstate, Chicago, IL, USA) and fluorescein isothiocyanate-labeled anti-BrdU (Becton Dickinson, Franklin Lakes, NJ, USA). Secondary antibodies used were Alexa Fluor 488 anti-mouse (Molecular Probes, Carlsbad, CA, USA) or HRP-conjugated goat anti-mouse and HRP-conjugated rabbit anti-goat (Dako, Glostrup, Denmark).

References

- Aleem E, Kiyokawa H, Kaldis P. (2005). Cdc2-cyclin E complexes regulate the G1/S phase transition. *Nat Cell Biol* **7**: 831–836.
- Alevizopoulos K, Vlach J, Hennecke S, Amati B. (1997). Cyclin E and c-Myc promote cell proliferation in the presence of p16INK4a and of hypophosphorylated retinoblastoma family proteins. *EMBO J* **16**: 5322–5333.
- Baus F, Gire V, Fisher D, Piette J, Dulic V. (2003). Permanent cell cycle exit in G2 phase after DNA damage in normal human fibroblasts. *EMBO J* **22**: 3992–4002.
- Benjamini Y, Hochberg Y. (1995). Controlling the false discovery rate: a practical and powerful approach to multiple testing. *J R Stat Soc B* **57**: 289–300.
- Blagosklonny MV, Pardee AB. (2002). The restriction point of the cell cycle. *Cell Cycle* **1**: 103–110.
- Brugarolas J, Bronson RT, Jacks T. (1998). p21 is a critical CDK2 regulator essential for proliferation control in Rb-deficient cells. *J Cell Biol* **141**: 503–514.
- Campbell SL, Khosravi-Far R, Rossman KL, Clark GJ, Der CJ. (1998). Increasing complexity of Ras signaling. *Oncogene* **17**: 1395–1413.
- Chang HY, Sneddon JB, Alizadeh AA, Sood R, West RB, Montgomery K *et al.* (2004). Gene expression signature of fibroblast serum response predicts human cancer progression: similarities between tumors and wounds. *PLoS Biol* **2**: E7.
- D'Abaco GM, Hooper S, Paterson H, Marshall CJ. (2002). Loss of Rb overrides the requirement for ERK activity for cell proliferation. *J Cell Sci* **115**: 4607–4616.
- Dannenbergh JH, van Rossum A, Schuijff L, te Riele H. (2000). Ablation of the retinoblastoma gene family deregulates G(1) control causing immortalization and increased cell turnover under growth-restricting conditions. *Genes Dev* **14**: 3051–3064.
- Dudley DT, Pang L, Decker SJ, Bridges AJ, Saltiel AR. (1995). A synthetic inhibitor of the mitogen-activated protein kinase cascade. *Proc Natl Acad Sci USA* **92**: 7686–7689.
- Fan S, Ma Y, Gao M, Yuan R, Meng Q, Goldberg I *et al.* (2001). The multisubstrate adapter Gab1 regulates hepatocyte growth factor (scatter factor)-c-Met signaling for cell survival and DNA repair. *Mol Cell Biol* **21**: 4968–4984.
- Feng J, Tamaskovic R, Yang Z, Brazil DP, Merlo A, Hess D *et al.* (2004). Stabilization of Mdm2 via decreased ubiquitination is mediated by protein kinase B/Akt-dependent phosphorylation. *J Biol Chem* **279**: 35510–35517.
- Foijer F, te Riele H. (2006a). Check, double check: the G2 barrier to cancer. *Cell Cycle* **5**: 831–836.
- Foijer F, te Riele H. (2006b). Restriction beyond the restriction point: mitogen requirement for G2 passage. *Cell Div* **1**: 8.
- Foijer F, Wolthuis RM, Doodeman V, Medema RH, te Riele H. (2005). Mitogen requirement for cell cycle progression in the absence of pocket protein activity. *Cancer Cell* **8**: 455–466.
- Guo Q, Malek R, Kim S, Chiao C, He M, Ruffly M *et al.* (2000). Identification of c-Myc responsive genes using rat cDNA microarray. *Cancer Res* **60**: 5922–5928.
- Hanahan D, Weinberg RA. (2000). The hallmarks of cancer. *Cell* **100**: 57–70.
- Harper JW, Adami GR, Wei N, Keyomarsi K, Elledge SJ. (1993). The p21 Cdk-interacting protein Cip1 is a potent inhibitor of G1 cyclin-dependent kinases. *Cell* **75**: 805–816.
- Hay N. (2005). The Akt-mTOR tango and its relevance to cancer. *Cancer Cell* **8**: 179–183.
- Iyer VR, Eisen MB, Ross DT, Schuler G, Moore T, Lee JC *et al.* (1999). The transcriptional program in the response of human fibroblasts to serum. *Science* **283**: 83–87.
- Knight ZA, Gonzalez B, Feldman ME, Zunder ER, Goldenberg DD, Williams O *et al.* (2006). A pharmacological map of the PI3-K family defines a role for p110alpha in insulin signaling. *Cell* **125**: 733–747.
- Malumbres M, Barbacid M. (2001). To cycle or not to cycle: a critical decision in cancer. *Nat Rev Cancer* **1**: 222–231.
- Medema RH, Kops GJ, Bos JL, Burgering BM. (2000). AFX-like forkhead transcription factors mediate cell-cycle regulation by Ras and PKB through p27kip1. *Nature* **404**: 782–787.
- Meijer L, Borgne A, Mulner O, Chong JP, Blow JJ, Inagaki N *et al.* (1997). Biochemical and cellular effects of roscovitine, a potent and selective inhibitor of the cyclin-dependent kinases CDC2, CDK2 and CDK5. *Eur J Biochem* **243**: 527–536.
- Morisaki H, Fujimoto A, Ando A, Nagata Y, Ikeda K, Nakanishi M. (1997). Cell cycle-dependent phosphorylation of p27 cyclin-dependent kinase (CDK) inhibitor by cyclin E/CDK2. *Biochem Biophys Res Commun* **240**: 386–390.
- Nakayama K, Nagahama H, Minamishima YA, Miyake S, Ishida N, Hatakeyama S *et al.* (2004). Skp2-mediated degradation of p27 regulates progression into mitosis. *Dev Cell* **6**: 661–672.
- Nigg EA. (2001). Mitotic kinases as regulators of cell division and its checkpoints. *Nat Rev Mol Cell Biol* **2**: 21–32.
- Oster S, Ho C, Soucie E, Penn L. (2002). *Advances in Cancer Research*. Academic Press, Elsevier Science & Technology Books: The Netherlands, pp 81–154.
- Peeper DS, Dannenberg JH, Douma S, te Riele H, Bernards R. (2001). Escape from premature senescence is not sufficient for oncogenic transformation by Ras. *Nat Cell Biol* **3**: 198–203.
- Sage J, Mulligan GJ, Attardi LD, Miller A, Chen S, Williams B *et al.* (2000). Targeted disruption of the three Rb-related genes leads to loss of G(1) control and immortalization. *Genes Dev* **14**: 3037–3050.
- Sarbassov DD, Ali SM, Sabatini DM. (2005). Growing roles for the mTOR pathway. *Curr Opin Cell Biol* **17**: 596–603.
- Smits VA, Klomp maker R, Arnaud L, Rijkse n G, Nigg EA, Medema RH. (2000a). Polo-like kinase-1 is a target of the DNA damage checkpoint. *Nat Cell Biol* **2**: 672–676.
- Smits VA, Klomp maker R, Vallenius T, Rijkse n G, Makela TP, Medema RH. (2000b). p21 inhibits Thr161 phosphorylation of Cdc2 to enforce the G2 DNA damage checkpoint. *J Biol Chem* **275**: 30638–30643.
- Sturn A, Quackenbush J, Trajanoski Z. (2002). Genesis: cluster analysis of microarray data. *Bioinformatics* **18**: 207–208.
- Theodosiou A, Ashworth A. (2002). MAP kinase phosphatases. *Genome Biol* **3**: reviews3009.1–reviews3009.10.

- Toyoshima H, Hunter T. (1994). p27, a novel inhibitor of G1 cyclin-CDK protein kinase activity, is related to p21. *Cell* **78**: 67–74.
- Valledor AF, Comalada M, Xaus J, Celada A. (2000). The differential time-course of extracellular-regulated kinase activity correlates with the macrophage response toward proliferation or activation. *J Biol Chem* **275**: 7403–7409.
- Yang YH, Dudoit S, Luu P, Lin DM, Peng V, Ngai J *et al.* (2002). Normalization for cDNA microarray data: a robust composite method addressing single and multiple slide systematic variation. *Nucleic Acids Res* **30**: e15.
- Zhou BP, Liao Y, Xia W, Spohn B, Lee MH, Hung MC. (2001). Cytoplasmic localization of p21Cip1/WAF1 by Akt-induced phosphorylation in HER-2/neu-overexpressing cells. *Nat Cell Biol* **3**: 245–252.
- Zhu H, Nie L, Maki C. (2005). Cdk2-dependent inhibition of p21 stability via a C-terminal cyclin-binding motif. *J Biol Chem* **280**: 29282–29288.

Supplementary Information accompanies the paper on the Oncogene website (<http://www.nature.com/onc>).